Chapter 20

Neutrino Interactions Beyond the Standard Model

20.1 Introduction

The phenomenon of neutrino oscillation discussed in Chapter 18 implies that neutrinos have finite mass. The phenomenology of neutrino oscillation determines only the mass square differences $\Delta m^2_{ij}(i \neq j)$ but not the absolute masses of the neutrinos. The scalar and fermionic structure of the standard model does not allow neutrinos to have non-zero mass. There is also the possibility that neutrinos may have magnetic moments (intrinsic or transition) considerably larger than the prediction of the standard model. Moreover, there are anomalous results in the measurements of neutrino and antineutrino oscillation parameters in various regions of energies which suggest that the standard model description in terms of three weak flavor doublets of leptons and quarks is not adequate to describe weak interactions and there may exist additional flavor of neutrinos which are non-interacting i.e. sterile. All these processes suggest that although the standard model has been a spectacular success in describing most electroweak processes, there is need for physics beyond the standard model.

Moreover, there are many other rare physical processes driven by weak interactions which have been studied for a long time theoretically as well as experimentally and are not explained by the standard model. The experimental observations of these processes would establish the physics beyond the standard model. The subject of physics beyond the standard model is too vast to be described in space of a chapter but we discuss here, some of the neutrino processes to introduce the subject.

(i) Neutrinoless double beta decay (NDBD) and Majorana neutrinos

(ii) Lepton flavor violating (LFV) decays of elementary particles

(iii) Flavor changing neutral current (FCNC)

(iv) Existence of non-standard interaction in high precision weak processes.

https://doi.org/10.1017/9781108489065.021 Published online by Cambridge University Press

20.2 Netrinoless Double-beta Decay

20.2.1 General considerations

The problem of double-beta decays (DBD) involving two-neutrino double-beta decay ($2\nu\beta\beta$) and neutrinoless double-beta decay ($0\nu\beta\beta$) has been with us for more than 80 years after it was first discussed by Goeppert-Mayer in the case of $(2\nu\beta\beta)$ in 1935 [1062] soon after the Fermi theory of β-decay was formulated [23] and the process of $0\nu\beta\beta$ was discussed by Furry in 1939[1063] after a new theory of neutrino was given by Majorana [121].

There are many nuclei in which ordinary β-decay, that is, $(A, Z) \rightarrow (A, Z+1) + e^- + \bar{\nu}_e$ is not allowed but the process of $2\nu\beta\beta$ decay $(A, Z) \rightarrow (A, Z+2) + e^- + e^- + \bar{\nu}_e + \bar{\nu}_e$ is kinematically allowed. This process occurs in the second order of weak interactions in which two nucleons decay simultaneously with the nucleus giving rise to two antineutrinos and two electrons, thus, involving five particle phase space in the final state as shown in Figure 20.1(a). The process is allowed in the standard model and the transition matrix element is proportional to $(G_F \cos\theta_C)^2$. Although the process is very rare, it has been observed in many nuclei with lifetimes in the range exceeding $10^{18} - 10^{19}$ years (see Table 20.1)[1064].

Table 20.1 Some of the measured values of $T^{2\nu}_{1/2}$ in various nuclei.

Isotope	$T^{2\nu}_{1/2}$ years	Isotope	$T^{2\nu}_{1/2}$ years
^{48}Ca	$4.4^{+0.6}_{-0.5} \times 10^{19}$	^{116}Cd	$(2.8 \pm 0.2) \times 10^{19}$
^{76}Ge	$(1.5 \pm 0.1) \times 10^{21}$	^{128}Te	$(1.9 \pm 0.4) \times 10^{24}$
^{82}Se	$(0.92 \pm 0.07) \times 10^{20}$	^{130}Te	$6.8^{+1.2}_{-1.1} \times 10^{20}$
^{96}Zr	$(2.3 \pm 0.2) \times 10^{19}$	^{150}Nd	$(8.2 \pm 0.9) \times 10^{18}$
^{100}Mo	$(7.1 \pm 0.4) \times 10^{18}$	^{150}Nd–^{150}Sm(0^+_1)	$1.33^{+0.45}_{-0.26} \times 10^{20}$
^{100}Mo–^{100}Ru(0^+_1)	$5.9^{+0.8}_{-0.6} \times 10^{20}$	^{238}U	$(2.0 \pm 0.6) \times 10^{21}$

Soon after the new theory of neutrino was proposed by Majorana in which the neutrino was considered to be its own antiparticle, Furry analyzed the $0\nu\beta\beta$ decay mode of nuclei in which the Racah sequence [1065], that is,

$$\begin{aligned} (A, Z) &\rightarrow (A, Z+1) + e^- + \bar{\nu}_e \\ \nu_e + A(Z+1) &\rightarrow A(Z+2) + e^- \\ \text{would lead to } (A, Z) &\rightarrow (A, Z+2) + e^- + e^- \end{aligned} \tag{20.1}$$

in case of virtual neutrinos as shown in Figure 20.1(b), if the neutrino is its own antiparticle, that is, $\bar{\nu} = \nu$ assuming that it is a Majorana neutrino. The decay rates for both types of double-beta decays were calculated in the context of the Fermi theory. Since the $0\nu\beta\beta$ decays are favored by the phase space consideration, the lifetimes of these decays were found to be in the range of $10^{15} - 10^{16}$ years for $0\nu\beta\beta$ and $10^{18} - 10^{22}$ years for $2\nu\beta\beta$ decays based on the phase space consideration. Clearly, $0\nu\beta\beta$ decay should have been discovered first but this did not happen [1066]. This implies that the physics of $2\nu\beta\beta$ and $0\nu\beta\beta$ decays are completely

https://doi.org/10.1017/9781108489065.021 Published online by Cambridge University Press

different from each other. We now know that it does not happen in the standard model which will be explained now.

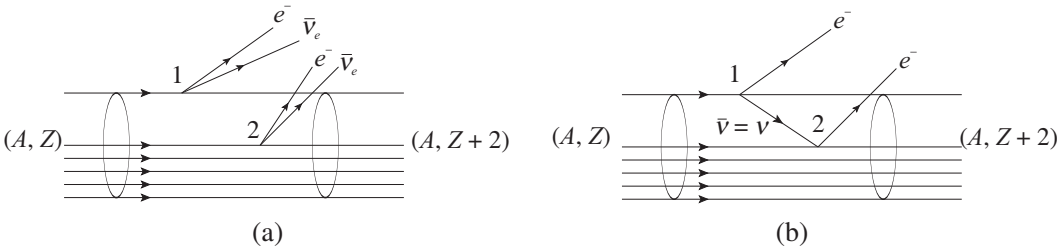

Figure 20.1 (a)$(A, Z) \rightarrow (A, Z+2) + e^- + e^- + \bar{\nu}_e + \bar{\nu}_e$ and (b)$(A, Z) \rightarrow (A, Z+2) + e^- + e^-$

At the first vertex in Figure 20.1(b), where an electron (e^-) is emitted, the electron is accompanied by an antineutrino which is right-handed, while the neutrino which is absorbed at the second vertex to produce the second electron, is left-handed. Thus, the process involves not only the condition that $\bar{\nu} = \nu$ but also that neutrino's helicity should flip. This process of $0\nu\beta\beta$ decay violates lepton number conservation by two units, that is, $\Delta L_e = 2$. It cannot happen for the massless neutrinos which conserve helicity. Therefore, in order that the Feynman diagram corresponding to Figure 20.1(b) gives a non-zero value of the transition matrix element, the neutrinos must have mass and the weak interaction must be lepton flavor violating (LFV) or both. The other alternative is to have additional interactions of Majorana neutrinos responsible for the flipping of the neutrino helicity. Both the possibilities may be present simultaneously. In both cases, we need to go beyond the standard model to describe the phenomenon of neutrinoless double-beta decay.

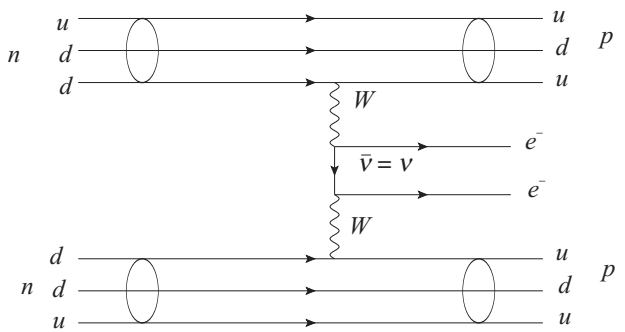

Figure 20.2 $nn \rightarrow pp + e^- + e^-$[1067].

There exist many theoretical models which have been proposed to generate the mass of Majorana neutrinos as well as theoretical models which predict new interactions for neutrinos by enlarging the $SU(2) \times U(1)$ group structure of the standard models like $SU(5), SO(10)$ or models based on super symmetry and have been applied to calculate the decay rates of neutrinoless double-beta decay of various nuclei. The subject has been presented in the classic review of Haxton et al. [1068] and Doi et al. [1069] as well as in many recent articles [1066, 1070, 1071, 1072, 1073] in view of the current interest in the phenomenology of neutrino

https://doi.org/10.1017/9781108489065.021 Published online by Cambridge University Press

oscillation with massive neutrinos. One of the simplest models is the left–right symmetric model having a minimal group structure of $SU(2)_L \times SU(2)_R \times U(1)$ allowing for right-handed currents which provide coupling to the opposite helicity Majorana neutrinos. Such models would have two sets of gauge bosons $W_L^{\pm}(Z_L)$ and $W_R^{\pm}(Z_R)$ coupling to the left-handed and right-handed lepton and quark current, that is, (j_μ^L, j_μ^R). The mass eigenstates of the gauge boson $W_1^{\pm}(Z_1)$ and $W_2^{\pm}(Z_2)$ would be the mixture of left-handed and right-handed gauge bosons $W_L^{\pm}(Z_L)$ and $W_R^{\pm}(Z_R)$ as

$$\begin{aligned} W_1^{\pm}(Z_1) &= W_L^{\pm}(Z_L)\cos\theta + W_R^{\pm}(Z_R)\sin\theta \\ W_2^{\pm}(Z_2) &= -W_L^{\pm}(Z_L)\sin\theta + W_R^{\pm}(Z_R)\cos\theta \end{aligned} \tag{20.2}$$

with $\theta < 1$ and $M_1 << M_2$ to reproduce the phenomenology of the standard model at the lower energy scale. There are many more sophisticated models of describing the physics beyond the standard model with more Higgs scalars or more gauge fields than in the SM gauge fields or heavy leptons, proposed in the context of the Grand Unified theories and supersymmetry (SUSY) which predict new interactions allowing the $0\nu\beta\beta$ decays.

Experimentally, there have been many attempts to search for $0\nu\beta\beta$ decays in various nuclei, which provide lower limits for their lifetime. The average mass of the electron neutrino generated by the neutrino mixing matrix parameters is estimated from these limits on the $0\nu\beta\beta$ decay lifetime of nuclei. A summary of such experiments [1074, 1075, 1076, 1077, 1078, 1079, 1080, 1081, 1082, 1083, 1084] is given in Table 20.2. Some of these experiments are being updated while new experiments are also planned.

Table 20.2 $T_{1/2}^{0\nu}$ and $\langle m_{\beta\beta}\rangle$ limits (90% C.L.) from the most recent experiments on $0\nu\beta\beta$ in various nuclei.

Isotope	$T_{1/2}^{0\nu}$ ($\times 10^{25}$ years)	$\langle m_{\beta\beta}\rangle$ (eV)	Experiment	Reference
^{48}Ca	$> 5.8 \times 10^{-3}$	$< 3.5 - 22$	ELEGANT-IV	[1074]
^{76}Ge	> 8.0	$< 0.12 - 0.26$	GERDA	[1075]
	> 1.9	$< 0.24 - 0.52$	MAJORANA DEMONSTRATOR	[1076]
^{82}Se	$> 3.6 \times 10^{-2}$	$< 0.89 - 2.43$	NEMO-3	[1066]
^{96}Zr	$> 9.2 \times 10^{-4}$	$< 7.2 - 19.5$	NEMO-3	[1077]
^{100}Mo	$> 1.1 \times 10^{-1}$	$< 0.33 - 0.62$	NEMO-3	[1078]
^{116}Cd	$> 1.0 \times 10^{-2}$	$< 1.4 - 2.5$	NEMO-3	[1079]
^{128}Te	$> 1.1 \times 10^{-2}$	—	—	[1080]
^{130}Te	> 1.5	$< 0.11 - 0.52$	CUORE	[1081]
^{136}Xe	> 10.7	$< 0.061 - 0.165$	KamLAND-Zen	[1082]
	> 1.8	$< 0.15 - 0.40$	EXO-200	[1083]
^{150}Nd	$> 2.0 \times 10^{-3}$	$< 1.6 - 5.3$	NEMO-3	[1084]

There are other processes equivalent to neutrinoless double beta-decays discussed earlier, which are also possible, depending on the nuclear structure of various nuclei and kinematical considerations $\beta^+\beta^+$ decays,

$$(A, Z) \rightarrow (A, Z-2) + e^+ + e^+ + \nu_e + \nu_e,$$

https://doi.org/10.1017/9781108489065.021 Published online by Cambridge University Press

the electron capture (EC) processes:

$$e^- + (A, Z) \quad \rightarrow \quad (A, Z-2) + e^+$$

and double electron capture (EC/EC) processes:

$$2e^- + (A, Z) \quad \rightarrow \quad (A, Z-2).$$

It should be noted that a possible $0\nu\beta\beta$ decay of the EC/EC type needs an additional particle in the final state to conserve energy and momentum which shold be emitted from the final nuclear state in order to be physically possible. These processes are difficult to observe but provide a strong motivation for studying the physics beyond the standard model.

20.2.2 Decay rates of $0\nu\beta\beta$

In a general description of weak interaction the $0\nu\beta\beta$ decay involving two neutrinos in the nucleus is depicted at the quark level as shown in Figure 20.2. In the simplest extension of the standard model based on the left–right symmetric models, the general Hamiltonian for $0\nu\beta\beta$ decay at the quark level (Figure 20.2) can be written as [1067]

$$\mathcal{H} = \frac{G_F \cos\theta_c}{\sqrt{2}} (l_L^\mu J_{L\mu}^\dagger + \kappa l_L^\mu J_{R\mu}^\dagger + \eta l_R^\mu J_{L\mu}^\dagger + \lambda l_{\mu R}^\mu J_{\mu R}^\dagger) \tag{20.3}$$

$$\text{where } l_{L,R}^\mu = \bar{e}\gamma^\mu(1-\gamma_5)\nu_{e_L}, \; l_R^\mu = \bar{e}\gamma^\mu(1+\gamma_5)\nu_{e_R} \tag{20.4}$$

$$J_L^\mu = \bar{u}_e\gamma^\mu(1-\gamma_5)d; \quad J_R^\mu = \bar{u}\gamma^\mu(1+\gamma_5)d. \tag{20.5}$$

In the standard model $k = \eta = \lambda = 0$, while in the left–right symmetric models,

$$\eta = k \approx \tan\theta, \quad \lambda \approx \left(\frac{M_1}{M_2}\right)^2 + \tan^2\theta$$

$$\text{leading to } \mathcal{H}^\beta = G_F \cos\theta\sqrt{2}\left[(\bar{e}_L\gamma_\mu\nu_{eL})\left(J_{L\mu}^\dagger + \eta J_{R\mu}^\dagger\right) + (\bar{e}_R\gamma_\mu\nu_{eR})\left(\eta J_{L\mu}^\dagger + \lambda J_{R\mu}^\dagger\right) + h.c.\right], \tag{20.6}$$

and

$$W_L = \cos\theta W_1 - \sin\theta W_2, \quad W_R = \sin\theta W_1 + \cos\theta W_2, \tag{20.7}$$

with $\eta = \tan\theta$ describing the mixing of $(W_L(Z))$ and $(W_R(Z))$ bosons as given in Eq. (20.2). The matrix elements of the nucleonic current $J_{\mu,L}^\dagger$ and $J_{\mu,R}^\dagger$, corresponding to FIg 20.1(b) are defined as (Chapter 10), where the sum over i is performed over the number of nucleons in the nucleus

$$J_L^{\mu\dagger} = \sum_i \bar{u}_p(i)\left[f_1(q^2)\gamma^\mu + i f_2(q^2)\frac{\sigma^{\mu\nu}}{2M_p}q_\nu - g_1(q^2)\gamma^\mu\gamma_5 - g_3(q^2)q^\mu\gamma_5\right]u_n(i), \tag{20.8}$$

for the left-handed nucleon currents, in which the form factors $f_j(q^2)$ $(j = 1, 2)$ and $g_j(q^2)$ $(j = 1, 3)$, are known and

$$J_R^{\mu\dagger} = \sum_i \bar{u}_p(i)\left[f_1'(q^2)\gamma^\mu + i f_2'(q^2)\frac{\sigma^{\mu\nu}}{2M_p}q_\nu + g_1'(q^2)\gamma^\mu\gamma_5 + g_3'(q^2)q^\mu\gamma_5\right]u_n(i), \tag{20.9}$$

https://doi.org/10.1017/9781108489065.021 Published online by Cambridge University Press

for the right-handed currents. The form factors $f_j(q^2)$ and $g_j(q^2)$ appearing in the matrix elements of the left- handed currents in Eq. (20.8) are discussed in Chapter 10.

It should be realized that while the bare couplings of the right-handed leptonic and hadronic currents in Eq. (20.9) are determined by the coefficients k, η, and λ, the form factors $f_j'(q^2)$ and $g_j'(q^2)$, appearing in the matrix elements of the right-handed currents $f_j'(g_j')$ are related with $f_j(q^2)$ and $g_j(q^2)$ defined for the left-handed currents as they are derived from the bare couplings due to the renormalization in the presence of strong interactions which conserve parity and therefore would be same as the form factors in the left handed current.

The process of $(0\nu\beta\beta)$ occurs in the second order as shown in Figure 20.1(b) and the decay rate is given by

$$dW \approx 2\pi \int |\mathcal{M}^{fi}|^2 \delta(E_f - E_i - E_{e_1} - E_{e_2}) F(Z, E_{e1}) F(Z, E_{e2}) d^3p_1 d^3p_2, \quad (20.10)$$

where $F(Z, E_{e1})$ and $F(Z, E_{e2})$ are the Fermi functions describing the Coulomb distortion of electrons in the field of final nucleus given in Chapter 5. $\mathcal{M}^{fi}$ is the transition matrix element calculated in the second order of perturbation theory leading to

$$\mathcal{M}^{fi} = L^{\mu\nu} J^{fi}_{\mu\nu}, \quad (20.11)$$

where $L^{\mu\nu}$ and $J_{\mu\nu}$ are the leptonic and hadronic tensors calculated by using the leptonic and hadronic currents l^μ and J_μ defining the interaction Hamiltonian given in Eq. (20.3). Without going into the details of calculation, we demonstrate the main features of particles physics and nuclear physics which enter into these calculations [1033].

Leptonic component

In calculating the second order of the matrix elements, the leptonic part depends on the product of two neutrino fields at space–time points x_1 and x_2 in Figure 20.1(b) which are contracted, leading to the lepton tensor given by reference of Engel and Menendez [1071] and Bilenky [1033]

$$\begin{aligned} L^{\mu\nu} &\propto \int\int dx_2 dx_1 \sum_i \bar{e}_L(x_1)\gamma^\mu(1-\gamma_5)U_{ei}\,\underline{\nu_{iL}(x_1)\bar{e}_L(x_2)\gamma^\nu(1-\gamma_5)U_{ei}\nu_{iL}(x_2)} \\ &= -\int\int dx_2 dx_1 \sum_i \bar{e}(x_1)\gamma^\mu(1-\gamma_5)U_{ei}\,\underline{\nu_{iL}(x_1)\bar{\nu}^c_{iL}}(x_2)\gamma_\nu(1+\gamma_5)U_{ei}e^C_L(x_2), \quad (20.12) \end{aligned}$$

where ν_i are the Majorana mass eigenstates with mass m_i and U_{ei} are the matrix elements of the mixing matrix. $\bar{\nu}_{iL}$ is the charge conjugate of the neutrino field which is equal to the neutrino field in the case of Majorana neutrinos $\nu_i^c = \nu_i$, where for a fermion field $\psi^C(x) = i\gamma^2\psi^*(x)$. The contraction of neutrino fields $\nu_{eL}(x_1)$ and $\bar{\nu}_{eL}(x_2)$ therefore gives the neutrino propagator leading to the leptonic tensor

$$\begin{aligned} L^{\mu\nu} \propto \int\int dx_1 dx_2 \Big[\sum_i \frac{d^4q}{(2\pi)^4} e^{-iq\cdot(x_1-x_2)} \bar{u}_e(p_1)\gamma_\mu(1-\gamma_5)e^{+i(p_1\cdot x_1 + p_2\cdot x_2)} \\ \frac{\not{q} + m_i}{q^2 - m_i^2}\gamma_\nu(1+\gamma_5)u^c_e(p_2)U^2_{ei}\Big], \quad (20.13) \end{aligned}$$

where q is the four momentum of the initial neutrino and p_1 and p_2 are the momenta of the two electrons. Now, we consider the following case of the weak interaction models:

https://doi.org/10.1017/9781108489065.021 Published online by Cambridge University Press

(a) Models in which there are Majorana neutrinos with no right-handed currents; here, $\not{q}$ terms operating on the leptonic part, vanish. The propagator term then reduces to

$$\begin{aligned} \frac{m_i}{q^2 - m_i^2} &\propto \frac{m_i}{q^2} \quad \text{if } m_i^2 << q^2 \\ &\propto -\frac{1}{m_i} \quad \text{if } m_i^2 >> q^2. \end{aligned} \tag{20.14}$$

implying that in the case of light neutrinos, the contribution to the transition matrix element for the leptonic part has different mass (m_i) and q^2 dependence than the case of heavy neutrinos, depending upon the mass (m_i) of the virtual neutrino exchanged between the two nucleons in the nuclei. In the case of the light neutrino scenario, it depends upon the effective mass $m_{\beta\beta}$ of Majorana neutrinos, given by:

$$m_{\beta\beta} = \sum_i U_{ei}^2 m_i. \tag{20.15}$$

(b) Models with $V + A$ currents in which the leptonic currents have opposite chirality; here, one gets from the neutrino propagator, a term like

$$\frac{\not{q}}{q^2 - m_i^2} \rightarrow \frac{\not{q}}{q^2}, \; m_i^2 << q^2 \tag{20.16}$$

$$\rightarrow -\frac{\not{q}}{m_i^2}, \; m_i^2 > q^2, \tag{20.17}$$

In the light neutrino scenario there is no ν-mass dependence in the transition matrix element.

It is worth emphasizing that in all the scenarios discussed till now, the kinematics becomes different and the neutrino mass plays a very important role. Since the mass m_i of Majorana neutrinos are yet to be determined experimentally, theoretical modeling of Majorana masses have been a very active field of physics beyond the standard model in recent years, in the context of $0\nu\beta\beta$ decays.

Hadronic component

The hadronic part of the matrix element $J_{\mu\nu}^{if}$ is calculated by taking the matrix element of the T-product $T(J_\mu(x_1)J_\nu(x_2))$ between the nuclear states $|i\rangle$ and $|f\rangle$, that is, [1033]

$$\begin{aligned} J_{\mu\nu}^{fi} &= \langle f|TJ_\mu(x_1)J_\nu(x_2)|i\rangle, \\ J_{\mu\nu}^{fi} &= \langle f|J_\mu(x_1)J_\nu(x_2)\theta(x_{1_0} - x_{2_0})|i\rangle + \langle f|J_\nu(x_2)J_\mu(x_1)\theta(x_{2_0} - x_{1_0})|i\rangle. \end{aligned} \tag{20.18}$$

Considering the first term, where $x_{1_0} > x_{2_0}$, after saturating it with a set of intermediate states $|n\rangle$, we write

$$J_{\mu\nu}^{if} = \sum_n \langle f|J_{\mu L}(x_1)|n\rangle\langle n|J_{\nu L}(x_2)|i\rangle + (\mu \rightarrow \nu, x_{1_0} \rightarrow x_{2_0}), \tag{20.19}$$

https://doi.org/10.1017/9781108489065.021 Published online by Cambridge University Press

where $|n\rangle$ is a complete set of intermediate states, that is, $\sum_n |n\rangle\langle n| = 1$.

$$J_\mu(x) = e^{iHx_0} J_{\mu L}(\vec{x}) e^{-iHx_0} \tag{20.20}$$

$$J^{fi}_{\mu\nu} = \sum_n \langle f|J_{\mu L}(\vec{x}_1)|n\rangle\langle n|J_{\nu L}(\vec{x}_2)|i\rangle e^{-i(E_n-E_f)x_{10}} e^{-i(E_n-E_i)x_{20}} + (\mu \to \nu, x_{10} \to x_{20}). \tag{20.21}$$

Now the matrix element $M^{fi} = L^{\mu\nu} J^{fi}_{\mu\nu}$ is evaluated using Eq. (20.11) and combining the various factors in Eq. (20.13) and (20.21); we integrate first over x_{10} and x_{20} and then integrate over q_0 to obtain the factor $2\pi\delta(E_f + E_{e_1} + E_{e_2} - E_i)$ and we get the following expression:

$$\begin{aligned} M^{fi}_{0\nu} \propto & \left(\frac{G_F^2 \cos^2\theta_C}{\sqrt{2}} \bar{u}(p)\gamma^\mu\gamma^\nu(1+\gamma^5)u^c(p_2)\right) \int d^3x_1 \int d^3x_2 e^{i(\vec{p}_1\cdot\vec{x}_1 + \vec{p}_2\cdot\vec{x}_2)} \\ & \sum_i U^2_{ei} m_i \int \frac{e^{i\vec{q}\cdot(\vec{x}_1-\vec{x}_2)}}{(2\pi)^3 q_i^0} d^3\vec{q}\, 2\pi\delta(E_f + p_1^0 + p_2^0 - E_i) \\ \times & \sum_n \left[\frac{\langle f|J_{\mu L}(\vec{x}_1)|n\rangle\langle n|J_{\nu L}(\vec{x}_2)|i\rangle}{E_n + p_2^0 + q_i^0 - E_i} + \frac{\langle f|J_{\nu L}(\vec{x}_2)|n\rangle\langle n|J_{\mu L}(\vec{x}_1)|i\rangle}{E_n + p_1^0 + q_1^0 - E_i}\right]. \end{aligned} \tag{20.22}$$

The matrix element in Eq. (20.22) is further evaluated, making the following approximations for the nucleons in nuclei and the kinematics of the virtual neutrinos and nucleons

1. The mass of the neutrinos are small, therefore, the energy $q_i^0 = \sqrt{|q_i|^2 + m_i^2} \simeq |\vec{q}_i|$. Since the virtual neutrinos are confined within the volume of the nuclei, with radius $\approx$ few fm, $|\vec{q}_i|$ is of the order of $\frac{1}{r}(= 100$ MeV).

2. The order of the magnitude of the momenta of the electrons emitted in the double beta-decay is a few MeV and the nuclear radius is about a few fm; therefore, the magnitude of $\vec{p}_1\cdot\vec{x}_1 \approx \vec{p}_2\cdot\vec{x}_2 \approx p\cdot R$ is very small of the order of 10^{-2} and the factor $e^{i(\vec{p}_1\cdot\vec{x}_1 + \vec{p}_2\cdot\vec{x}_2)} \approx 1$.

3. The evaluation of the nuclear matrix element M_{fi} requires the knowledge of the nuclear ground state of the initial nucleus as well as the excited states of the final nucleus. Since the energy of virtual neutrinos could be of the order of 100 MeV almost all the excited states $|n\rangle$ need to be considered. This is not easy. Therefore, nuclear matrix elements are evaluated in closure approximation. For this, we assume an average excitation energy $\bar{E}$ for E_n, so that the summation over $|n\rangle$ states could be performed assuming the completeness relation. Therefore, we write:

$$\sum_n \frac{\langle f|J_\mu(\vec{x}_1)|n\rangle\langle n|J_\nu(\vec{x}_2)|i\rangle}{E_n + p_2^0 + q_i^0 - E_i} \simeq \frac{\langle f|J_\mu(x_1)J_\nu(x_2)|i\rangle}{\bar{E} + p_2^0 + |\vec{q}| - E_i}, \tag{20.23}$$

$$\sum_n \frac{\langle f|J_\nu(\vec{x}_2)|n\rangle\langle n|J_\mu(\vec{x}_1)|i\rangle}{E_n + p_1^0 + q_i^0 - E_i} \simeq \frac{\langle f|J_\nu(x_2)J_\mu(x_1)|i\rangle}{\bar{E} + p_1^0 + |\vec{q}| - E_i}. \tag{20.24}$$

https://doi.org/10.1017/9781108489065.021 Published online by Cambridge University Press

4. Neglecting nuclear recoil, we can write:

$$E_i \;=\; E_f + p_1^0 + p_2^0 = \frac{E_i + E_f}{2} + \frac{p_1^0 + p_2^0}{2}$$

implying

$$|\vec{q}| + \bar{E} + p_{1,2}^0 - E_i \;=\; |\vec{q}| + \bar{E} - \frac{E_i + E_f}{2} \pm \frac{(p_1^0 - p_2^0)}{2}. \tag{20.25}$$

Since $\frac{p_1^0 - p_2^0}{2}$ is much smaller than other terms, the denominator in both terms is the same and depends only upon $\vec{q}$, making it easier to perform d^3q integration in Eq. (20.22), because $J_\mu(x)J_\nu(y)$ is independent of q in the leading order (as given here in Eq. (20.29)). Therefore, performing the $\vec{q}$ integration leads to

$$\frac{1}{(2\pi)^3}\int \frac{e^{iq|\vec{x}_1 - \vec{x}_2|}d^3q}{q(q + \bar{E} - \frac{1}{2}(E_i + E_f))} = \frac{1}{2\pi^2 r}\int \frac{\sin qr\, dq}{q + \bar{E} - \frac{E_i + E_f}{2}} = \frac{1}{4\pi R}H(r, \bar{E}), \tag{20.26}$$

with $\vec{r} = |\vec{x}_1 - \vec{x}_2|$ and R being the nuclei radius.

such that $H(r, \bar{E}) = \frac{2R}{\pi r}\int_0^\infty \frac{\sin qrdq}{q + \bar{E} - \frac{1}{2}(E_i + E_f)}$ which is called the neutrino potential.

5. The weak interaction current operator $J^\mu(x)$ in the nuclei is calculated in the impulse approximation using nonrelativistic nucleons (Chapter 14). In this approximation,

$$J_{0L}(\vec{x}) \;\simeq\; \sum_i \delta(\vec{x} - \vec{x}_i) f_1(0)\tau_i^+ \tag{20.27}$$

$$\vec{J}_L(\vec{x}) \;\simeq\; \sum_i \delta(\vec{x} - \vec{x}_i) g_1(0)\vec{\sigma}_i\tau_i^+ \tag{20.28}$$

in the lower order, where $\sum_i$ is over nucleons such that

$$J_{\mu L}(\vec{x}_1)J_{\nu L}(\vec{x}_2) = \sum_{i,j}\tau_i^+\tau_j^+\delta(\vec{x}_1 - \vec{x}_i)\delta(\vec{x}_2 - \vec{x}_j)[f_1^2(0) - g_1^2(0)\vec{\sigma}_i \cdot \vec{\sigma}_j]. \tag{20.29}$$

Note that because of Eqs. (20.27) and (20.28), only $\mu = 0, \nu = 0$ and $\mu = i, \nu = j$ components contribute in the leptonic part $L^{\mu\nu}$. The matrix element in Eq. (20.22) is therefore written as:

$$M_{0\nu}^{fi} \;\propto\; 2\pi\delta(E_f - E_i - E_1 - E_2)\left(\frac{G_F \cos\theta_C}{\sqrt{2}}\right)^2 m_{\beta\beta}$$

$$\times\; \bar{u}(p_1)(1 + \gamma^5)u^c(p_2)M_{0\nu}, \tag{20.30}$$

where $M_{0\nu} \;=\; f_1^2(0)M_{0\nu}^F - g_1^2(0)M_{0\nu}^{GT}$

$$M_{0\nu}^F \;=\; \langle f|\sum_{i,j} H(r_{ij}, \bar{E})\tau_i^+\tau_j^+|i\rangle \tag{20.31}$$

$$M_{0\nu}^{GT} \;=\; \langle f|\sum_{i,j} H(r_{ij}, \bar{E})\vec{\sigma}_i \cdot \vec{\sigma}_j\tau_i^+\tau_j^+|i\rangle \tag{20.32}$$

https://doi.org/10.1017/9781108489065.021 Published online by Cambridge University Press

and $m_{\beta\beta}$ is given by Eq. (20.15). Using this value of $M_{0\nu}$ in Eq. (20.30), the square of the matrix element $\sum_{\text{leptons}} |M_{0\nu}^{fi}|^2$ is calculated as:

$$\sum_{\text{leptons}} |M_{0\nu}^{fi}|^2 \propto \left(\frac{G_F \cos\theta_C}{\sqrt{2}}\right)^4 m_{\beta\beta}^2 \, 8p_1 \cdot p_2 |M_{0\nu}|^2, \tag{20.33}$$

using $\sum_{\text{spins}} |\bar{u}(p_1)(1+\gamma^5)u(p_2)|^2 = 8p_1 \cdot p_2$.

Nuclear matrix elements $M_{0\nu}$

All the nuclei which are likely candidates for neutrinoless β-decay are heavy nuclei (far from the closed shell); some of them are also deformed nuclei. Therefore, the theoretical calculation of the nuclear matrix element is a formidable nuclear problem. The different approaches used for calculating the nuclear matrix elements (NME) are the nuclear shell model (NSM) and the quasi particle random phase approximation (QRPA) [1068, 1069]. Recently, calculations based on the projected Hartree–Fock–Bogoliobov (PHFB) model, the interacting boson model (IBM), and the energy density functional (EDF) methods have also been used [1070, 1071, 1072, 1073, 1068, 1069].

In the closure approximation, the NME depends upon the nuclear wave functions and on the neutrino potential $H(r)$ given in Eq. (20.26) arising due to the virtual neutrino propagator which is of long range. The calculation of $M_{0\nu}$ requires a very good knowledge of nuclear wave function in the entire range of r, and the various nuclear structure models give different results. Moreover, in the case of calculations using multipole expansion (Chapter 14), the sum over various multipoles has a very slow convergence. Since the energy of the virtual neutrinos could be of the order of 100 MeV, there are many multipoles which contribute. This necessitates a good knowledge of almost all the excited state wave functions of the final nucleus, making the calculations of NME very difficult. It is because of this reason that closure approximation is used (see Chapter 14) Moreover, in the case of particle physics models based on $0\nu\beta\beta$ decays mediated by heavy neutrinos or other heavy particles, the short range correlation effects in the nuclear wave functions make the calculations of NME even more difficult.This leads to considerable uncertainty in the results for NME [1071, 1067, 1085], Various calculations could give results differing from each other by a factor of 2-3. For details, see Engel and Menendez [1071].

There is some experimental information available on the nuclear wave functions in the case of a few nuclei in which $2\nu\beta\beta$ decays have been observed. The experimental strength of GT transitions for $0^+ \rightarrow 1^+$ transitions is also available in some nuclei from the $(^2\text{He}, d)$ and $(^3\text{He}, t)$ reactions. In the case of transitions involving ground states, limited information is also available from electron capture and muon capture experiments. However, these are limited in scope and describe very few excitations corresponding to the low lying excited states in the final nucleus. In summary, the NME are the major source of uncertainty in the study of $0\nu\beta\beta$ decays.

https://doi.org/10.1017/9781108489065.021 Published online by Cambridge University Press

Phase space and decay rates

The decay rate is obtained using Eqs. (20.11), (20.30) and (20.33) after integrating the $\sum|M^{fi}|^2$, over the phase space of two electrons. The phase space is considerably modified in the presence of the Coulomb field of the nucleus (A, Z+2). Therefore, the decay rate is given by [1067]:

$$\begin{aligned}\Gamma_{o\nu} &= m_{\beta\beta}^2|M_{o\nu}|^2\int_{m_e}F(E_1,Z+2)F(E_2,Z+2)\frac{d^3p_1}{2E_1(2\pi)^3}\frac{d^3p_2}{2E_2(2\pi)^3}\\ &\times\ 8(E_1E_2-|\vec{p}_1||\vec{p}_2|\cos\theta)2\pi\delta(E_f-E_i-E_1-E_2)\\ &= m_{\beta\beta}^2|M_{o\nu}|^2G(Q,Z),\end{aligned}\tag{20.34}$$

where

$$\begin{aligned}G(Q,Z) &\propto \int\int F(E_1,Z+2)F(E_2,Z+2)|\vec{p}_1||\vec{p}_2|(E_1E_2-|\vec{p}_1||\vec{p}_2|\cos\theta)dE_1dE_2\\ &\quad\delta(Q-E_1-E_2),\end{aligned}\tag{20.35}$$

and $Q\approx M_i-M_f-2m_e$, neglecting the nuclear recoil. $m_{\beta\beta}$ and $|M_{o\nu}|^2$ are given in Eqs. (20.15) and (20.33) and $|\vec{p}_1|(|\vec{p}_2)$ are the magnitude of 3-momenta $\vec{p}_1(\vec{p}_2)$.

In the case of other particle physics models, the decay rate has many more terms; for example, in the minimal extension of the standard model having the right-handed currents based on $SU(2)_L\times SU(2)_R\times U(1)$, the decay rate in Eq. (20.34) is now given by [1067]:

$$\begin{aligned}\Gamma^{o\nu} &= C_{mm}\frac{m_{\beta\beta}^2}{m_e^2}+C_{\eta\eta}\langle\eta\rangle^2+C_{\lambda\lambda}\langle\lambda\rangle^2\\ &\quad+C_{m\eta}\left(\frac{m_{\beta\beta}}{m_e}\right)\langle\eta\rangle+C_{m\lambda}\left(\frac{m_{\beta\beta}}{m_e}\right)\langle\lambda\rangle+C_{\eta\lambda}\langle\eta\rangle\langle\lambda\rangle,\end{aligned}\tag{20.36}$$

where $\langle\eta\rangle=\eta\sum_i U_{ei}V_{ei}$, $\langle\lambda\rangle=\lambda\sum_i U_{ei}V_{ei}$ with V_{ej} as the mixing matrix elements among the right-handed neutrino states. Equation (20.36) reduces to Eq. (20.34) when $\langle\eta\rangle$, $\langle\lambda\rangle=0$ in the standard model. For example, the element C_{mm} becomes

$$C_{mm}=|M_{0\nu}|^2G(Q,Z)m_e^2.\tag{20.37}$$

20.2.3 Experiments

The experimental observation of the neutrinoless double beta-decay is very challenging as it is perhaps the smallest theoretically predicted process accessible to observation after the proton decay. The typical energy for a double beta-decay is of the order of a few MeV, which is shared by four leptons in the case of $2\nu\beta\beta$ and two electrons in the case of $0\nu\beta\beta$ decay. The decay spectrum of the two electrons as a function of $E_e=E_{e_1}+E_{e_2}$ is a delta function in the case of $0\nu\beta\beta$; the decay rate has Q^5 dependence. Therefore, amongst the heavy nuclei which are likely candidates of $0\nu\beta\beta$decay, only those with larger Q value and larger nuclear matrix element for the transitions are favored for experimental studies. The list of several such nuclei which have been studied is given in Table 20.2. Since this is a very rare process, a significant amount of source material should be made available either naturally or by isotopical enrichment Moreover, a low-level counting technique for detecting charged particles should be

https://doi.org/10.1017/9781108489065.021 Published online by Cambridge University Press

used along with sufficient arrangements made for shielding from background events. The major sources of background are charged particles produced by cosmic rays and by the natural and artificial radioactivity in the surrounding material leading to charged particles through primary or secondary interactions. In this scenario, the deep underground experiments planned for the study of proton decays and atmospheric neutrinos are the most sutaible laboratories for performing DBD (double beta-decay) experiments in both modes of $2\nu\beta\beta$ and $0\nu\beta\beta$ decays. Since $0\nu\beta\beta$ decay is a rarer process compared to $2\nu\beta\beta$ decays by at least 5–6 orders of magnitude, the charged particles from $2\nu\beta\beta$ are themselves a serious background. However, their energy spectra are quite different from the electrons from $0\nu\beta\beta$ decays.

There is an extensive experimental program being pursued for the study of DBD which started in 1948 and also focussed on $0\nu\beta\beta$ decay in early years using Geiger, proportional, and scintillation counters using few grams of source material. These days, sophisticated detectors of various types with considerable high energy resolution are being used with hundreds of kilograms of source material. These are categorized according to various techniques used for the detection of signals of charged particles. Excellent reviews of the experimental developments are given by many reviewers [1070, 1068, 1069, 1086, 1087, 1088]. In the following, we present a summary of various experiments without describing them individually. The details of each experiment mentioned below can be found in the above references and Giuliani et al. [1089].

Semiconductor detectors

High purity germanium (HPGe) detectors enriched with ^{76}Ge are the most suitable detectors in the source as detector configuration for studying $0\nu\beta\beta$ decays and have been used in the Hydelberg-Moscow and IGEX experiments as well as in the current generation of GERDA and Majorana DEMONSTRATOR experiments in underground laboratories at Gran Sasso, Aquila Italy and Sanford, Lead USA. The results for the upper limits for $0\nu\beta\beta$ lifetimes for various nuclei from these experiments are already available and are shown in Table 20.2. The upgrades of GERDA have shown the technical feasibility of doing large scale $0\nu\beta\beta$ decay experiments and the experiments proposed at LEGEND-200 and LEGEND-1000 with 200 and 1000 kg of enriched ^{76}Ge.

Cryogenic detectors

Bolometers are cryogenic calorimeters that operate at very low temperatures of $\approx$ 10 mK. A heat absorber is connected via a weak thermal link to a low temperature thermal bath and the increase in temperature due to the energy deposited by the charge particles produced in $0\nu\beta\beta$ is measured by a sensitive thermometer. A variety of materials with $\beta\beta$ emitting nuclei like ^{130}Te, ^{116}Cd, ^{82}S, ^{100}Mo can be used as bolometric absorbers. Experiments like CUORE-O, Coricino, and CUORE use enriched ^{130}Te source from which experimental limits are already available (Table 20.2). The upgrade of CUORE like CUPID with ^{100}Mo and ^{82}Se $\beta\beta$ emitters are planned at LNGS, Italy in the near future. Other advanced detectors of this type are AMORE-I and AMORE-II planned to be operated in South Korea with 5 kg and 200 kg of ^{100}Mo crystals as source material with sensitivity up to $10^{25} - 10^{26}$ years for the β lifetime of ^{100}Mo, which is an improvement by a factor of 10–100 from the present limits.

https://doi.org/10.1017/9781108489065.021 Published online by Cambridge University Press

Scintillator detectors

Another type of detectors which have been used in the source–detector configuration are the scintillators detector. The advantage of these detectors is that they can be used with $\beta\beta$ emitters with higher values of Q like ^{48}Ca. The latest detector in this category is the ELEGANT-IV setup in Japan providing limits on $0\nu\beta\beta$ decays lifetime for ^{48}Ca(Table 20.2). The series of CANDLES detectors using ^{48}Ca have been used to carry out experiments at the Kamioka Observatory. The latest in the series of CANDLES-III detectors have already reported early results for their experiment. In another experiment, ^{116}Cd was used in the Solotvino salt mine in Ukraine to obtain an upper limit on the lifetime of ^{116}Cd (1.7×10^{23} years).

In addition to these detector experiments based on inorganic scintillators, KamLAND-ZEN and SNO+ detectors use ^{136}Xe and ^{130}Te $\beta\beta$ emitters in large liquid scintillators. The KamLAND-ZEN loaded with 320 kg and 400 kg enriched ^{136}Xe has already reported results (Table 20.2) and an update to KamLAND-II with 1 ton ^{136}Xe is already planned. Another experiment, ZICOS loaded with 45 kg of liquid scintillator enriched ^{96}Zr is also being planned.

Ionization detectors

Experiments based on these detectors are called passive experiments and use the principle of ionizations and scintillations and make use of time projection chambers (TPC). The $\beta\beta$ emitter is used in the form of gas or thin foils; the emitted electrons are tracked in energy and angle between electrons. In most of the experiments, ^{136}Xe has been used or is planned to be used. EXO-200 with 110 kg of enriched ^{136}Xe has already produced limits on ^{136}Xe lifetime against $0\nu\beta\beta$ and updates like nEXO with 500 kg of ^{136}Xe is already planned. Other experiments with ^{136}Xe like NEXT-100 with 100 kg of ^{136}Xe in Spain and PandaX with 200 kg of ^{136}Xe in China, are already planned for future operations.

Tracking calorimeter detectors

Tracking calorimeter detectors like NEMO-3 situated in the Frejus laboratory in France use a thin foil of source material surrounded by a gas tracking layer in which two electrons are tracked in energy and the angle between them. It has been used to report limits on the $0\nu\beta\beta$ lifetime of ^{100}Mo,^{116}Co,^{82}Se, and ^{96}Zr. The SuperNEMO experiment, an update of the NEMO-3 plans to use 20 modules containing 6.3 kg of ^{82}Se in each module to be surrounded by scintillator blocks to track the electrons and is projected to reach a half life sensitivity of $\approx 10^{26}$ years, that is, an improvement by a factor 10^2 on the present limits.

The observation of NDBD will establish the mass of the neutrino and its Majorana nature in the context of theoretical developments and confirm the existence of a physics beyond the standard model (BSM). However, there are many theoretical models formulated for describing the physics beyond the standard model like Grand Unified Theories (GUT), string theory, supersymmetry (SUSY) and others in which the neutrino masses and new interactions are predicted depending upon the parameters of the model. We would, therefore, need more experiments with greater sensitivity to BSM physics in order to find the correct theoretical description of the physics beyond the standard model.

https://doi.org/10.1017/9781108489065.021 Published online by Cambridge University Press

20.3 Lepton Flavor Violating Processes

There are many other leptonic, hadronic, and nuclear processes, which are allowed if the lepton flavor number is not conserved as in the case of the neutrinoless double beta decay (NDBD). The predictions for the rates of these processes are based on various theories using beyond the standard model (BSM) physics. In NDBD, the electron lepton number L_e is violated by two units, that is, $\Delta L_e = 2$, but there could be processes in which the muon lepton number L_μ is violated with one or more units as well as the processes in which L_e and L_μ, both are violated. All these processes have the capability of discriminating among the various models of the BSM physics. Such processes are predicted in $\Delta S = 0$ as well as in $\Delta S = 1$ sectors involving muons and electrons.

The leptonic processes involving heavy leptons $\mu^{\pm}(\tau^{\pm})$ in which these particles decay into lighter leptons $e^{\pm}(\mu^{\pm})$ without any neutrinos, violate L_e, L_μ or both and are not allowed in the standard model. The observation of such processes is a signature of BSM physics. The present limits on many leptonic processes with lepton flavor violation (LFV) [1090] are given in Table 20.3.

Table 20.3 Table for rare leptonic processes with lepton flavour violation (LFV).

Decay mode	Present limit	Decay mode	Present limit
$\mu^- \to e^-\gamma$	$< 1.2 \times 10^{-11}$	$\mu^-\mathrm{Ti} \to e^-\mathrm{Ti}$	$< 6.1 \times 10^{-13}$ (PSI)
$\mu^+ \to e^+e^+e^-$	$< 1.0 \times 10^{-12}$	$\mu^-\mathrm{Ti} \to e^-\mathrm{Ti}$	$< 4.6 \times 10^{-12}$ (TRIUMF)
$\mu^+e^- \to \mu^-e^+$	$< 8.3 \times 10^{-11}$	$\mu^- + \mathrm{Cu} \to e^+ + \mathrm{Co}$	$< 2.6 \times 10^{-8}$
$\tau \to e\gamma$	$< 2.7 \times 10^{-6}$	$\mu^- + \mathrm{S} \to e^+ + \mathrm{Si}$	$< 9 \times 10^{-10}$
$\tau \to \mu\gamma$	$< 3 \times 10^{-6}$	$\mu^-\mathrm{Au} \to e^-\mathrm{Au}$	$< 7 \times 10^{-13}$ (SINDRUM)
$\tau \to \mu\mu\mu$	$< 1.9 \times 10^{-16}$		
$\tau \to eee$	$< 2.9 \times 10^{-6}$		

These processes can be calculated using the two-body or three-body kinematics for decay and scattering processes described elsewhere in the book provided that the interaction Lagrangians are known. There are various calculations done for these processes with phenomenological Lagrangians based on theoretical models to describe the physics beyond the standard model. Among the theoretical models, supersymmetry (SUSY) models have received much attention. Minimal supersymmetry models (MSSM), SUSY with explicit symmetry breaking and R-parity violation or SUSY models proposed in context of Grand Unified Theories (GUT) have been used extensively in literature to calculate these processes. Theoretical models based on the right-handed neutrinos, charged Higgs bosons, more gauge fields than SM gauge fields and leptoquarks have also been used.

There are also LFV decay processes involving pions, kaons, or Z bosons which have been searched for the presence of BSM physics. Some of these processes with present limits are listed in Table 20.4. They can also be calculated in the models proposed for BSM physics and would be able to discriminate between various models if they are observed experimentally.

https://doi.org/10.1017/9781108489065.021 Published online by Cambridge University Press

Table 20.4 Rare hadronic processes with lepton flavor violation (LFV).

Decay mode	Limit on branching ratio	Decay mode	Limit on branching ratio
$\pi^0 \to \mu e$	$< 8.6 \times 10^{-9}$	$D^+ \to \pi^- e^+ e^+$	$< 3.6 \times 10^{-6}$
$K_L^0 \to \mu e$	$< 4.7 \times 10^{-12}$	$D^+ \to \pi^- \mu^+ \mu^+$	$< 4.8 \times 10^{-6}$
$K^+ \to \mu^+ \mu^- e^-$	$< 2.1 \times 10^{-10}$	$D^+ \to \pi^- e^+ \mu^+$	$< 5.0 \times 10^{-5}$
$K_L^0 \to \pi^0 \mu^+ e^-$	$< 3.1 \times 10^{-9}$	$D_s^+ \to \pi^- e^+ e^+$	$< 6.9 \times 10^{-4}$
$Z^0 \to \mu e$	$< 1.7 \times 10^{-6}$	$D_s^+ \to \pi^- \mu^+ \mu^+$	$< 2.9 \times 10^{-5}$
$Z^0 \to \tau e$	$< 9.8 \times 10^{-6}$	$D_s^+ \to \pi^- e^+ \mu^+$	$< 7.3 \times 10^{-4}$
$Z^0 \to \tau \mu$	$< 1.2 \times 10^{-5}$	$B^+ \to \pi^- e^+ e^+$	$< 1.6 \times 10^{-6}$
$K^+ \to \pi^- e^+ e^+$	$< 6.4 \times 10^{-10}$	$B^+ \to \pi^- \mu^+ \mu^+$	$< 1.4 \times 10^{-6}$
$K^+ \to \pi^- \mu^+ \mu^+$	$< 3.0 \times 10^{-9}$	$B^+ \to \pi^- e^+ \mu^+$	$< 1.3 \times 10^{-6}$
$K^+ \to \pi^- e^+ \mu^+$	$< 5.0 \times 10^{-10}$		

20.4 Flavor Changing Neutral Currents

We have seen in earlier chapters that the suppression of FCNC induced by $s \to d$ and $b \to s$ transitions at the quark level was a special feature of the standard model (SM). These processes could occur through higher order loop diagrams in the standard model with fine tuning of heavy flavor quark masses (Figure 20.3). These processes are also predicted in many extensions of the SM (Figure 20.4) like the Z, Z' models, leptoquark models, MSSM models with various extensions. An experimental observation of such decays would play an important role in studying the BSM physics.

20.4.1 Particle decay processes

FCNC processes are driven by quark level transitions like $s \to d\nu\bar{\nu}$ and $b \to s\nu\bar{\nu}$. Some of the FCNC processes in the strangeness sector that involve neutrinos are $K^\pm \to \pi^\pm \nu\bar{\nu}$, $K_L^0 \to \pi^0 \nu\bar{\nu}$. Processes like $K^\pm \to \pi^+ e^\pm \mu^\mp$ and $K^- \to \pi^- e^\pm \mu^\mp$ involve FCNC as well as the lepton flavor violation (LFV) with $|\Delta L_e| = |\Delta L_\mu| = 1$. Processes like $K^\pm \to \pi^\pm \nu\bar{\nu}$ and $K_L^0 \to \pi^0 \nu\bar{\nu}$ can occur in the standard model through the higher order loop diagrams involving $W(Z)$ bosons and/or u, c, t quarks in the intermediate state (Figure 20.3). Preliminary results from the NA62 experiment from CERN (Table 20.5) has generated great excitement in the study of these reactions; forthcoming experiments at JPARC would play a decisive role in studying the FCNC processes [1091].

The new contributions from BSM physics would add to the standard model contribution either coherently or incoherently, depending upon the structure of the model which could have

i) Additional quarks or gauge bosons or Higgs (Figure 20.4(a)).

ii) Additional light neutrinos ν_R or sterile neutrinos ν_S (Figure 20.4(b)).

iii) New interaction with lepton flavor violation (LFV) (Figure 20.4(c)).

iv) Leptoquark (Figure 20.4(d)).

https://doi.org/10.1017/9781108489065.021 Published online by Cambridge University Press

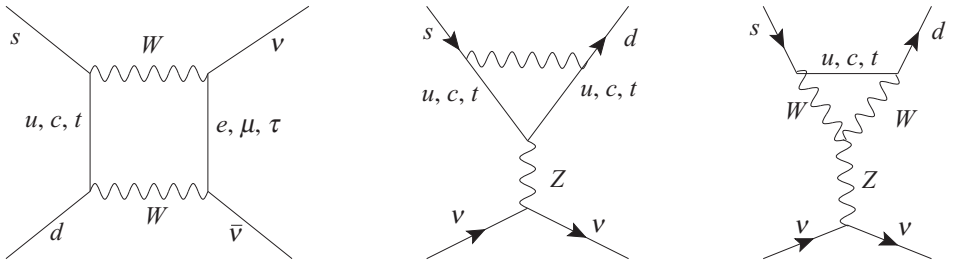

Figure 20.3 Flavor changing neutral current processes in higher order loop diagrams in SM.

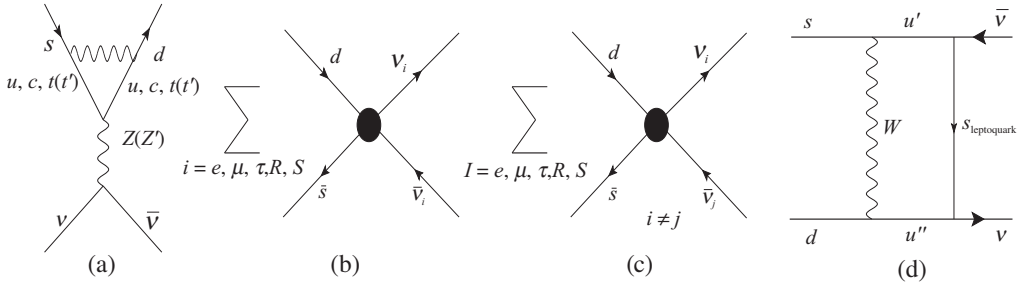

Figure 20.4 Flavor changing neutral current processes in some models beyond the standard model (BSM) physics.

Since the two neutrinos in the final state are not observed, these contributions would modify the decay rates. The existence of new particles and new interactions envisaged in the BSM physics models are constrained to satisfy well-established observations on the number of light neutrinos from LEP, that is, $n = 2.9840 \pm 0.0082$ or the limits on the strength of right-handed

Table 20.5 Recent experimental limits of FCNC kaon decays.

Decay mode	Present limit	Experiment
$K^+ \to \pi^+ \nu\bar{\nu}$	$< 1.85 \times 10^{-10}$	NA62 (2019)
	$< 2.88 \times 10^{-10}$	BNL787
$K^+ \to \pi^+ e^- \mu^+$	$< 1.3 \times 10^{-11}$	BNL 865

current couplings or the coupling of new Higgs or Z bosons. These BSM physics models are also applied to predict the rates for other FCNC decays like $K^\pm \to \pi^\pm e^+ \mu^-$ and $K^\pm \to \pi^\pm e^- \mu^+$.

20.4.2 Production of strange and heavy flavored hadrons in scattering experiments

The presence of FCNC can be experimentally tested in various scattering experiments induced by neutrinos, electrons, or in $e^- e^+$ collisions at LEP. In the low energy region, where MINERvA operates, the observation of processes like

https://doi.org/10.1017/9781108489065.021 Published online by Cambridge University Press

$$\begin{aligned} \nu + p &\rightarrow \nu + \Sigma^+ \\ \nu + n &\rightarrow \nu + \Lambda^0\ (\Sigma^0) \end{aligned}$$

or at the electron accelerators at JLAB and MAINZ [1092, 1093], processes like

$$\begin{aligned} e^- + p &\rightarrow e^- \Sigma^+ \\ e^- + D &\rightarrow e^- \Lambda^0 p \\ e^- + D &\rightarrow e^- n \Sigma^+ \end{aligned} \tag{20.38}$$

could be searched for. In the very high energy region of LEP, the search for single top quark productions or leptoquark production induced by FCNC have been made. Any observation of such events would give information about the BSM physics through the study of FCNC.

20.5 Nonstandard Interaction (NSI) in High Precision Low Energy Weak Processes

In recent years, there has been remarkable progress in high precision experiments at very low energies involving nuclear and neutron β decays. This has renewed interest in examining the low energy effects of BSM in high precision weak processes at low energies. These efforts involve probing for the presence of exotic current couplings of scalar, tensor, pseudoscalar, and right-handed currents in β decays as well as the high precision study of symmetry properties of weak currents under discrete symmetries like parity (P), time reversal (T), charge conjugation (C), and CP symmetry [1094, 1095, 226, 1096]. Various beta decay parameters can be measured with high precision and the parameters which were earlier inaccessible or were measured with poor precision can be determined with high precision using polarized neutron and nuclear sources; these parameters can test various models proposed for physics beyond the standard model (BSM). In this low energy region, the weak interaction is described in terms of (u, d) quarks and (e, ν_e) and (μ, ν_μ) leptons. In the quark picture, the interaction Lagrangian $\mathcal{L}^{\text{eff}}$ for $d \rightarrow ue\nu$ including the nonstandard interactions can be written as [1094, 1095, 226]:

$$\begin{aligned} \mathcal{L}_{\text{eff}} = -\frac{G_F V_{ud}}{\sqrt{2}} \Big[& (1+\epsilon_L)\ \bar{e}\gamma_\mu(1-\gamma_5)\nu_e \cdot \bar{u}\gamma^\mu(1-\gamma_5)d \ +\ \tilde{\epsilon}_L\, \bar{e}\gamma_\mu(1+\gamma_5)\nu_e \cdot \bar{u}\gamma^\mu(1-\gamma_5)d \\ & + \epsilon_R\, \bar{e}\gamma_\mu(1-\gamma_5)\nu_e \cdot \bar{u}\gamma^\mu(1+\gamma_5)d \ +\ \tilde{\epsilon}_R\, \bar{e}\gamma_\mu(1+\gamma_5)\nu_e \cdot \bar{u}\gamma^\mu(1+\gamma_5)d \\ & + \epsilon_T\, \bar{e}\sigma_{\mu\nu}(1-\gamma_5)\nu_e \cdot \bar{u}\sigma^{\mu\nu}(1-\gamma_5)d \ +\ \tilde{\epsilon}_T\, \bar{e}\sigma_{\mu\nu}(1+\gamma_5)\nu_e \cdot \bar{u}\sigma^{\mu\nu}(1+\gamma_5)d \\ & + \epsilon_S\, \bar{e}(1-\gamma_5)\nu_e \cdot \bar{u}d \ +\ \tilde{\epsilon}_S\, \bar{e}(1+\gamma_5)\nu_e \cdot \bar{u}d \\ & - \epsilon_P\, \bar{e}(1-\gamma_5)\nu_e \cdot \bar{u}\gamma_5 d \ -\ \tilde{\epsilon}_P\, \bar{e}(1+\gamma_5)\nu_e \cdot \bar{u}\gamma_5 d \ +\ \ldots \Big] + \text{h.c.}\,, \end{aligned} \tag{20.39}$$

The aforementioned Lagrangian depicts the SM $(V-A)$ Fermi interaction, with

$$V_{ud} = \cos\theta_c. \tag{20.40}$$

https://doi.org/10.1017/9781108489065.021 Published online by Cambridge University Press

ϵ_i and $\tilde{\epsilon}_i$ are complex coefficients which are functions of the masses and couplings of the new particles and depend upon the detailed predictions of the models proposed for BSM. In general, these coefficients are expressed as:

$$\epsilon_i, \tilde{\epsilon}_i \propto \left(\frac{M_W}{\Lambda}\right)^2 , \tag{20.41}$$

where Λ is the energy scale of new physics (NP) and is of the order of $\Lambda \sim$TeV. This means that $\epsilon_i, \tilde{\epsilon}_i \approx 10^{-3}$ [226].

The Fermi constant, obtained from muon decay, phenomenologically, is $G_F = 1.1663787\,(6) \times 10^{-5}\,\text{GeV}^{-2}$. The Fermi coupling G_F is also determined from the nuclear β decays using mainly the Fermi decays induced by the vector currents which would get additional contributions due to ϵ_L and ϵ_R terms in Eq. (20.39). Neglecting the ϵ_i' terms as they involve right-handed neutrinos, we, therefore, write

$$\tilde{V}_{ud} \equiv V_{ud}\,(1 + \epsilon_L + \epsilon_R)\left(1 - \frac{\delta G_F}{G_F}\right) , \tag{20.42}$$

where δG_F is the change in G_F due to other corrections in SM and new physics (NP) due to BSM. The effective Lagrangian is rewritten to first order in ϵ_i as:

$$\begin{aligned}\mathcal{L}_{\text{eff}} \;=\; & -\frac{G_F \tilde{V}_{ud}}{\sqrt{2}}\Big\{\bar{e}\gamma_\mu(1-\gamma_5)\nu_e \cdot \bar{u}\gamma^\mu\left[1-(1-2\epsilon_R)\,\gamma_5\right] d \\ & + \epsilon_S\,\bar{e}(1-\gamma_5)\nu_e \cdot \bar{u}d - \epsilon_P\,\bar{e}(1-\gamma_5)\nu_e \cdot \bar{u}\gamma_5 d + \epsilon_T\,\bar{e}\sigma_{\mu\nu}(1-\gamma_5)\nu_e \cdot \bar{u} \\ & \sigma^{\mu\nu}(1-\gamma_5)d\Big\} + \text{h.c.}\end{aligned} \tag{20.43}$$

The matrix elements of the hadronic current in this equation between the nucleon states are defined as (Chapter 10)

$$\langle p(p_p)|\,\bar{u}\gamma_\mu d\,|n(p_n)\rangle = \bar{u}_p(p_p)\Big[f_1(q^2)\,\gamma_\mu + \frac{f_2(q^2)}{2M_N}\,\sigma_{\mu\nu}q^\nu + \frac{f_3(q^2)}{2M_N}\,q_\mu\Big]u_n(p_n), \tag{20.44a}$$

$$\langle p(p_p)|\,\bar{u}\gamma_\mu\gamma_5 d\,|n(p_n)\rangle = \bar{u}_p(p_p)\Big[g_1(q^2)\gamma_\mu + \frac{g_2(q^2)}{2M_N}\sigma_{\mu\nu}q^\nu + \frac{g_3(q^2)}{2M_N}q_\mu\Big]\gamma_5 u_n(p_n), \tag{20.44b}$$

$$\langle p(p_p)|\,\bar{u}\,d\,|n(p_n)\rangle = g_S(0)\;\bar{u}_p(p_p)\,u_n(p_n) + \mathcal{O}(q^2/M_N^2)\,, \tag{20.44c}$$

$$\langle p(p_p)|\,\bar{u}\,\gamma_5\,d\,|n(p_n)\rangle = g_P(0)\;\bar{u}_p(p_p)\,\gamma_5\,u_n(p_n) + \mathcal{O}(q^2/M_N^2), \tag{20.44d}$$

$$\langle p(p_p)|\,\bar{u}\,\sigma_{\mu\nu}\,d\,|n(p_n)\rangle = g_T(0)\;\bar{u}_p(p_p)\,\sigma_{\mu\nu}u_n(p_n) + \mathcal{O}(q/M_N), \tag{20.44e}$$

where $f_i(q^2), g_i(q^2)$ $(i = 1,2,3,S,P,T)$ are the form factors. It should be noted that $f_2(q^2)$, $f_3(q^2), g_2(q^2), g_3(q^2)$ are additional couplings induced by the strong interactions of nucleons which may get additional contributions from g_S, g_P, and g_T, which are new contributions due to NP only.

https://doi.org/10.1017/9781108489065.021 Published online by Cambridge University Press

In the limit $q^2 \to 0$, corresponding to β decays, in which only S,V,T,A,P form factors at $q^2 = 0$ make significant contributions (see Chapters 4 and 10), we can write

$$\begin{aligned} -\mathcal{L}_{n\to pe^-\bar{\nu}_e} &= \bar{p}\, n\, \left(C_S \bar{e}\nu_e - C'_S \bar{e}\gamma_5\nu_e\right) + \bar{p}\gamma^\mu n \left(C_V \bar{e}\gamma_\mu\nu_e - C'_V \bar{e}\gamma_\mu\gamma_5\nu_e\right) \\ &+ \frac{1}{2}\bar{p}\sigma^{\mu\nu} n \left(C_T \bar{e}\sigma_{\mu\nu}\nu_e - C'_T \bar{e}\sigma_{\mu\nu}\gamma_5\nu_e\right) - \bar{p}\gamma^\mu\gamma_5 n \left(C_A \bar{e}\gamma_\mu\gamma_5\nu_e - C'_A \bar{e}\gamma_\mu\nu_e\right) \\ &+ \bar{p}\gamma_5 n \left(C_P \bar{e}\gamma_5\nu_e - C'_P \bar{e}\nu_e\right) + \text{h.c.} \end{aligned} \tag{20.45}$$

where C_i and $C'_i (i = S, V, T, A, P)$ are expressed in terms of ϵ_i and $\tilde{\epsilon}_i (i = S, P, T, A, P)$. That is,

$$C_i(C'_i) = \frac{G_F \cos\theta_C}{\sqrt{2}} \bar{C}_i(\bar{C}'_i), \tag{20.46}$$

and $\bar{C}_i(\bar{C}'_i)$ are expressed in terms of ϵ_i and $\tilde{\epsilon}_i$ as [226]

$$\begin{aligned} \overline{C}_V + \overline{C}'_V &= 2 f_1 (1 + \epsilon_L + \epsilon_R) & \overline{C}_V - \overline{C}'_V &= 2 f_1 (\tilde{\epsilon}_L + \tilde{\epsilon}_R) \\ \overline{C}_A + \overline{C}'_A &= -2 g_1 (1 + \epsilon_L - \epsilon_R) & \overline{C}_A - \overline{C}'_A &= 2 g_1 (\tilde{\epsilon}_L - \tilde{\epsilon}_R) \\ \overline{C}_S + \overline{C}'_S &= 2 g_S \epsilon_S & \overline{C}_S - \overline{C}'_S &= 2 g_S \tilde{\epsilon}_S \\ \overline{C}_P + \overline{C}'_P &= 2 g_P \epsilon_P & \overline{C}_P - \overline{C}'_P &= -2 g_P \tilde{\epsilon}_P \\ \overline{C}_T + \overline{C}'_T &= 8 g_T \epsilon_T & \overline{C}_T - \overline{C}'_T &= 8 g_T \tilde{\epsilon}_T \,, \end{aligned} \tag{20.47}$$

The various observables studied in the β decays of polarized neutrons and polarized nuclei like the decay rates, angular and energy distributions of electrons (protons), various spin correlations between the spins of the decaying neutron and outgoing electrons and neutrinos, helicity of (anti)neutrino and polarization of electrons (positrons) etc. as discussed in Chapter 4, are used to determine the coefficients C_i and C'_i which would give the values of ϵ_L and ϵ_R. The SM without right handed currents $(\tilde{\epsilon}_i = 0)$ predicts that

$$C_V = C'_V, \;\; C_A = C'_A, C_i(C'_i) = 0 \quad (i \neq V, A). \tag{20.48}$$

The most recent values of these coupling constants assuming no right-handed currents are given in Table 20.6, with $|C_V| = 0.98554 \frac{G_F}{\sqrt{2}}$: The nuclear β decays do not give any limits

Table 20.6 Recent values of various couplings $C_i \; (i = V, A, S, T)$ determined from β decays which taken from [226].

$\text{Re}\left(\frac{C_A}{C_V}\right) = -1.27290(17)$	$\text{Im}\left(\frac{C_A}{C_V}\right) = -0.00034(59)$
$\text{Re}\left(\frac{C_S}{C_V}\right) = 0.0014(12)$	$\text{Im}\left(\frac{C_S}{C_V}\right) = -0.007(30)$
$\text{Re}\left(\frac{C_T}{C_V}\right) = 0.0020(22)$	$\text{Im}\left(\frac{C_T}{C_V}\right) = 0.0004(33)$

on C_P which is obtained from other probes using particle decays and production of hadrons in electroweak interactions, which also provide limits on C_T and C_S. From these values of C_i and

https://doi.org/10.1017/9781108489065.021 Published online by Cambridge University Press

C_i', limits on ϵ_i and $\tilde{\epsilon}_i$ are derived. Experiments in the high energy scattering experiments at LEP and LHC also provide limits on ϵ_i and $\tilde{\epsilon}_i$. Analysis with nonzero values for the right-handed current couplings are also performed in most of these β decay experiments; they are described in detail by Dolinski et al. [1070] and Cirigliano et al. [1094, 1095]. The bounds on scalar and tensor couplings for the β decays are $|\tilde{\epsilon}_S| < 0.0063$ and $0.006 < \tilde{\epsilon}_T < 0.024$. The limits from the other experiments at LEP and LHC on new interactions are:

$$|\epsilon_{S,P}|, |\tilde{\epsilon}_{S,P}| < 5.8 \times 10^{-3}; \qquad |\epsilon_T|, |\tilde{\epsilon}_T| < 1.3 \times 10^{-3}; \qquad |\epsilon_R| < 2.2 \times 10^{-3} \quad (20.49)$$

A discussion of these results is beyond the scope of this book.

20.6 Summary

The present experimental efforts in observing neutrinoless double beta decay in many nuclei leading to the sucessful observation of these decays will go a long way in determining the properties of neutrinos regarding their mass and nature of being Dirac or Majorana type. Various experimental efforts at LEP of producing tau particles and gauge bosons and their rare decays as well as the production of kaons and other hadrons with heavy flavor contents at CERN and their decay governed by FCNC processes will also provide valuable information in distinguishing among the different models of BSM physics. In the field of lepton physics, intense beams of muons to be made available at various laboratories may also help in observing many rare decays of muons and muon capture processes in nuclei with LFV. In view of this, we expect very exciting times in the study of BSM physics in the near future.

https://doi.org/10.1017/9781108489065.021 Published online by Cambridge University Press